

## Residual stress analysis with various thicknesses of Copper films by XRD

Research Article

Halo Dalshad Omar\*

Department of Physics, Faculty of Science and Health, Koya University, Koya KOY45, Kurdistan Region - ER. Iraq

Received 26 July 2019; accepted (in revised version) 20 August 2019

**Abstract:** In this study, investigation on the various thicknesses of Copper (Cu) film determined residual stress and ( $a_0$ ) lattice parameter by X-ray diffraction (XRD) technique. Copper films on plastic substrate at different thicknesses were elaborated at room temperature by sputtering deposition. The effect of the various thicknesses of the samples observers under strong compressive or tensile stress state by method  $\sin^2\psi$ . The diffraction peak position by  $\sin^2\psi$  were used to analysis the residual stress state. After that, strain can be measured by the residual stress. However, residual stress is inside a material without load on the samples.

**Keywords:** Residual stress • Method  $\sin^2\psi$  • Strain and XRD

© 2019 The Author(s). This is an open access article under the CC BY-NC-ND license (<https://creativecommons.org/licenses/by-nc-nd/3.0/>).

### 1. Introduction

The principle and fundamental of the methods to analysis residual stress and lattice parameter ( $a_0$ ) are described by XRD technique [1]. Mechanical characteristics like residual stresses for advanced coating technology. XRD is the most commonly used techniques to determine the residual stress, ( $a_0$ ) lattice parameter and strain into copper films on plastic substrate. The residual stress determined by  $\sin^2\psi$  law for Cu thin film with different thickness on plastic substrate [2, 3]. Sputtering deposition can be controlled the thickness under pressure vacuum.

In addition, residual stress is mean that it change of the lattice parameter of an isotropic formed by inter plane. Besides, the crystal structure of copper metallic is face center cubic and the arrangement of grain orientation of copper metallic and polycrystal line material.

### 2. Experimental details

Before deposition the substrate of plastic surface was cleaned chemically with acetone for a short time because substrate must be remove contaminants. The samples were fabricated by sputtering deposition. A thin film of Cu was elaborated into sputtering is performed with at a constant power  $P=200$  W, and constant time deposition  $t=120$  s, whereas the constant argon as a gas in a high vacuum system pressure is  $10^{-5}$  Pa at temperature  $250$  °C. Plastic substrates has an area  $(2\times 2)$  cm<sup>2</sup> with two thickness film approximately between 150 and 200 nm was measured by the weighting-method by a digital balance. XRD used to determine residual stress analysis was carried out using a diffractometer and operating at 40 kV and 40 mA, with a Cu X-ray tube  $\lambda = 0.154$  nm [4, 5]. The peak of Cu film (111), (200) and (220) are corresponding approximately peak position ( $2\theta$ ) to equal  $43.83^\circ$ ,  $50.84^\circ$  and  $74.62^\circ$  as shown in Fig. 1.

\* E-mail address: [halo.dalshad@koyauniversity.org](mailto:halo.dalshad@koyauniversity.org)

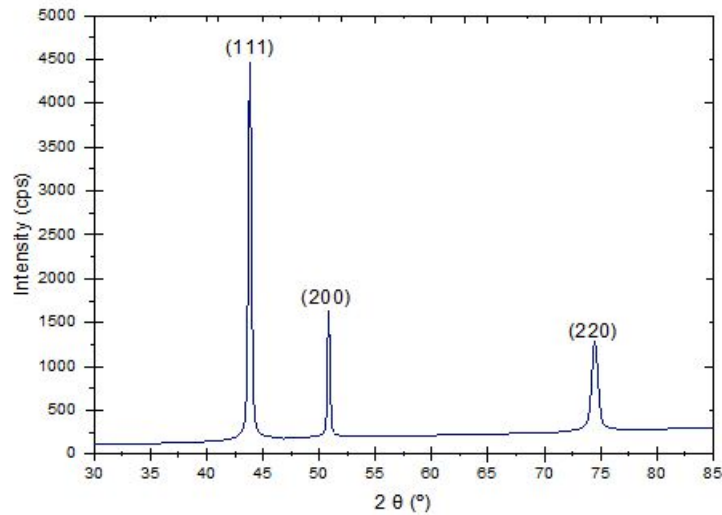


Fig. 1. Peak position of copper film on plastic by XRD

### 3. Result and discussion

#### 3.1. Residual Stress analysis

The measurement of residual stress by XRD; primarily, Cu on plastic has been observed as a shift in the location of the diffraction peaks and finds the peak position  $2\theta$ . XRD technique is based on the measurement of the angular shift of diffraction lines being caused by stresses. Residual stresses were determined by XRD using the method of  $\sin^2\psi$ . This method is based on measuring the variation of the position of the Bragg peak as a function of  $\sin^2\psi$ . In addition, there are three corrections intensity by defocusing, background and absorption correction because the intensity depends on the Bragg angle  $\theta$  (intensity lost from detector), the thick sample approximately between 150 nm and 200 nm and interaction with air and electronic noise. Besides, in Fig. 2 to determine the high intensity from  $\psi = 5^\circ$  to  $75^\circ$ . This shape was tensile stress and determined by  $\sin^2\psi$  versus  $\ln(1/\sin(\theta))$  for three peaks Cu on plastic substrate with 150 nm thickness. In Fig. 3 to determine the high intensity from  $\psi = 30^\circ$  to  $80^\circ$ . This shape was compressive stress and

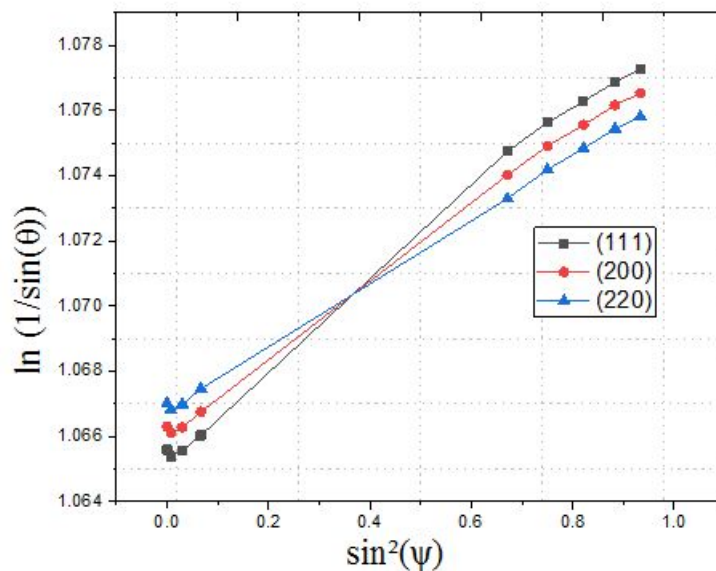


Fig. 2. Tensile stress analysis for Cu/ plastic substrate by XRD

determined by  $\sin^2\psi$  versus  $\ln(1/\sin(\theta))$  for three peaks Cu on plastic substrate with 200 nm thickness.

According to the theory a locally isotropic elasticity, the strain  $\varepsilon_{\phi\psi}$  in the direction of the vector  $L_3$  (azimuth  $\phi$  and

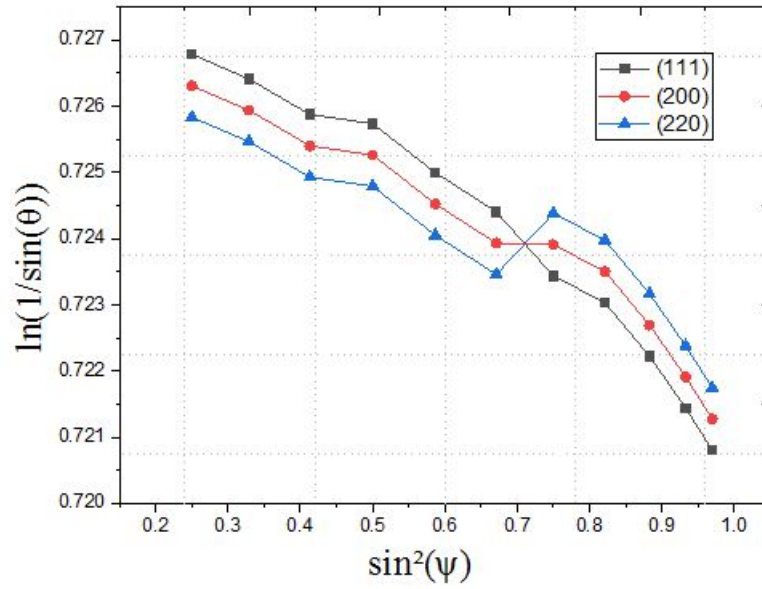


Fig. 3. Compressive stress analysis for Cu/ plastic substrate by XRD

$\psi$  polar angle) [2, 4, 6, 7].

$$\varepsilon_{L3} = \varepsilon_{\phi\psi} = \frac{1+\nu}{E} [\sigma_{11} \cdot \cos^2 \phi + \sigma_{12} \cdot \sin^2 \phi + \sigma_{22} \cdot \sin^2 \phi - \sigma_{33}] \sin^2 \psi + \frac{1+\nu}{E} \sigma_{33} - \frac{\nu}{E} [\sigma_{11} + \sigma_{22} + \sigma_{33}] + \frac{1+\nu}{E} [\sigma_{13} \cdot \cos \phi + \sigma_{23} \cdot \sin \phi] \sin 2\psi \quad (1)$$

Where  $E$  is Young's modulus,  $\nu$  is Poisson's ratio and  $\sigma_{11}, \sigma_{22}, \sigma_{33}, \sigma_{12}, \sigma_{13}, \sigma_{23}$  are stresses acting in the principal directions,  $\lambda$  is wave length,  $\theta$  is diffraction angle and  $d$  is interplaner lattice distance. The law of  $\sin^2 \psi$  is then given by the following expression [5, 6].

$$\varepsilon_{\phi\psi} = \ln \left( \frac{a_{hkl}}{a_0} \right) = \ln \left( \frac{d_{\phi\psi}}{d_0} \right) \approx \frac{d_{\phi\psi} - d_0}{d_0} = \ln \left( \frac{\sin \theta_0}{\sin \theta_\psi} \right) = \frac{1+\nu}{E} \sigma_{11} \sin^2 \psi - \frac{2\nu}{E} \sigma_{11} \quad (2)$$

Where  $d_{\phi\psi}$  (resp.  $d_0$ ) is the (resp. unstrained) lattice plane spacing of the  $hkl$  planes,  $\theta_\psi$  and  $\theta_0$  the angular positions of the corresponding diffraction peaks through Bragg's law and  $a_0$  being the stress-free lattice parameter and  $a_{hkl}$  the measured lattice parameter [8].

Linear adjustments of  $2\theta_{\phi\psi}$  evolution as a function of  $\sin^2 \psi$  allowed for determining both the residual stress (from the slope) and stress-free lattice parameter (from the intercept).

Assuming a state of plane stress exists, i.e.  $\sigma_{33} = 0$ , that the no shear stress are biaxial and the thickness thin films between 150 nm and 200 nm deposited on a substrate by sputtering [9].

$$\ln \left( \frac{1}{\sin \theta_\psi} \right) = \frac{1+\nu}{E} \sigma_{11} \sin^2 \psi - \frac{2\nu}{E} \sigma_{11} + \ln \left( \frac{1}{\sin \theta_0} \right) \quad (3)$$

For copper elastic constant ( $E = 130$  GP and  $\nu = 0.34$ )  $\sigma_{11} = \sigma_{22}$

To determine the residual stress  $\sigma_{11}$  and experimental and lattice constant  $a_0$  by Eq. (2):  $\sigma_{11} = 130$  GPa /  $(1 + 0.34) \times 0.00712 = 0.6907$  Gpa and  $a_0$  (lattice parameter) =  $3.605 \text{ \AA}$  (sample) >  $a_0 3.597 \text{ \AA}$  (theory) for (tensile stress) by Fig. 2.

$\sigma_{11} = 130$  GPa /  $(1 + 0.34) \times (-0.0080) = -0.7761$  Gpa and  $a_0$  (sample) =  $3.583 \text{ \AA}$  <  $a_0 = 3.597 \text{ \AA}$  theory for (compression stress) by Fig. 3.

#### 4. Strain analysis

The normal strain along the crystallographic plane normal direction can be measured by the  $2\theta$  shift of the diffraction pattern. Hook's laws give the linear relationships between strain and stress via the Young's modulus and Poisson's ratio [10–12]. With this hypothesis the relationship between stresses and strains become:

$$\varepsilon_{11} = \frac{1}{E} (\sigma_{11} - \nu \sigma_{22}), \varepsilon_{22} = \frac{1}{E} (\sigma_{22} - \nu \sigma_{11}) \quad \& \quad \varepsilon_{33} = -\frac{\nu}{E} (\sigma_{11} + \sigma_{22}) \quad (4)$$

$$\varepsilon_{12} = \varepsilon_{13} = \varepsilon_{23} = 0 \quad (5)$$

In the case of an equi-biaxial loading where  $\sigma_{11} = \sigma_{22} = \sigma$ , composites no zero macroscopic strain tensor can then be written:

$$\varepsilon_{11} = \varepsilon_{22} = \left( \frac{1-\nu}{E} \right) \sigma \quad (6)$$

$$\varepsilon_{33} = -\frac{2\nu}{E} \sigma \quad (7)$$

To determination strain for Cu on plastic with different thickness by the residual stress  $\sigma_{11}$  Eq. (7):

By the Eq. (7) calculate the strain for the Fig. 2 is a tensile stress.

$$\varepsilon_{11} = \varepsilon_{22} = (1 - 0.34/130) \times 0.6907 = 0.6888$$

$$\varepsilon_{33} = (-2 \times 0.34)/130 \times 0.6907 = -0.00361$$

By the Eq. (7) calculate the strain for the Fig. 3 is a compression stress.

$$\varepsilon_{11} = \varepsilon_{22} = (1 - 0.34/130) \times -0.7761 = -0.7740$$

$$\varepsilon_{33} = ((-2 \times 0.34)/130) \times -0.7761 = 0.5277$$

## 5. Conclusion

In this work, the influence of the thickness Cu film measured of the residual stress. In addition, Cu on plastic was used to deposit the coating. Cu thin films are determined to be formed by a face center cubic and have three peaks. The curves of residual stress difference shape were the tension and compression depend the technique deposition, thickness of the sample and some factors affected on the width diffracted peak by micro stress and the crystal structure such as plastic deformation, dislocation and vacancy in the Cu films during the deposition without load on the sample. To determination the value of residual stress calculated from the  $\ln(1/\sin(\theta))$ - $\sin^2\psi$  diagrams. The plotting  $\ln(1/\sin(\theta))$  versus  $\sin^2\psi$  is several angles for Figs. 2 and 3 and the difference in the shape of a curve for the Fig. 2 is tensile and the value is positive but in the Fig. 3 is compression and value is negative and the lattice parameter was depend the shape of the sample. Besides, strain can be measured by the stress for two samples.

## References

- [1] O. Anderoglu, Residual stress measurement using X-ray diffraction, Texas A&M University, 2005.
- [2] M. Fitzpatrick et al., Determination of residual stresses by X-ray diffraction, 2005.
- [3] C.-H. Ma, J.-H. Huang, H.J.T.S.F. Chen, Residual stress measurement in textured thin film by grazing-incidence X-ray diffraction 418(2) (2002) 73-78.
- [4] P.S.J.A.I. Prevey, ASM Handbook, X-ray diffraction residual stress techniques 10 (1986) 380-392.
- [5] P.S.J.D.i.M.C.T. Prevey, Current applications of X-ray diffraction residual stress measurement (1996) 103-110.
- [6] D. Hoffman, J.A.J.T.S.F. Thornton, The compressive stress transition in Al, V, Zr, Nb and W metal films sputtered at low working pressures 45(2)(1977) 387-396.
- [7] M. Smith, A.J.I.J.o.P.V. Smith, Piping, NeT bead-on-plate round robin: Comparison of residual stress predictions and measurements 86(1) (2009) 79-95.
- [8] Q. Luo, S. Yang, Uncertainty of the X-ray Diffraction (XRD)  $\sin^2\psi$  Technique in Measuring Residual Stresses of Physical Vapor Deposition (PVD) Hard Coatings, Coatings, 7(8) (2017) 128.
- [9] M. R. James, Recent Advances in the Measurement of Residual Stress by X-Ray Diffraction.
- [10] S.J. Skrzypek, A. Baczmanski, Progress in X-ray diffraction of residual macro-stresses determination related to surface layer gradients and anisotropy. Adv. X-ray Anal. 44 (2001) 134.
- [11] F. Barati et al., Buckling analysis of functionally graded beams with imperfectly integrated surface piezoelectric layers under low velocity 2(1) 92014) 64-73.
- [12] M. FarhadiNia et al., Analysis investigation of composite lattice conical shell as satellite carrier adapter for aerospace applications 1(4) (2014) 40-51.